Realization of an infrared spectral radiant power response scale on a cryogenic bolometer

A. Migdall and G. Eppeldauer

Abstract. The National Institute of Standards and Technology (NIST) has developed an infrared (IR) radiant power response scale for the spectral range from 2 μm to 20 μm. The scale has been realized on a cryogenic bolometer. The response of this bolometer has been determined by multiple ties to a primary standard, the NIST High Accuracy Cryogenic Radiometer (HACR). These transfers were made using three intermediate detectors over three different spectral regions. In addition, an independent method was used to determine the relative response of the bolometer over the entire spectral range. An IR spectral response scale over the entire 2 μm to 20 μm range was determined from these measurements, with the interlocking nature of the multiple independent measurements providing improved overall confidence and reduced uncertainties. The overall scale combined standard uncertainty for the entire spectral range of 2 μm to 20 μm is of the order of 0.25 %, with the typical combined standard uncertainty of an individual measurement made with the bolometer being ~0.8 %.

1. Introduction

The National Institute of Standards and Technology (NIST) has developed an IR radiant power response scale for the spectral range from 2 μm to 20 μm. This scale is required for a facility that provides a detector-based calibration of IR detector spectral radiant power response [1, 2]. The scale operates at much higher sensitivities (input power levels are 20 pW to 10 μW) than existing IR scales (~0.1 μW to 500 μW) [3], while using a detector with a flat spectral response over the entire spectral range. The scale has been realized on a cryogenic bolometer, which accounts for the improved sensitivity relative to a pyroelectric detector-based scale. The response of this bolometer has been determined by multiple ties to a primary standard, the NIST High Accuracy Cryogenic Radiometer (HACR) [4]. These transfers were made using three intermediate detectors over three different spectral regions. In addition, an independent method was used to determine the relative response of the bolometer over the entire spectral range. An overall IR spectral response scale was determined from these measurements, with the interlocking nature of the multiple independent measurements providing improved confidence and reduced uncertainty. The combined standard uncertainty over the entire spectral range of 2 μm to 20 μm is typically better than 0.25 %, with the typical uncertainty of an individual measurement made with the bolometer being ~0.8 %.

A. Migdall and G. Eppeldauer: Optical Technology Division, 221/B208, National Institute of Standards and Technology, Gaithersburg, MD 20899, USA.

2. Relative response determination

To determine the radiant power response of the bolometer, its relative response was predicted over its entire spectral range from measurements of bolometer components. This relative response shape was then tied down at many wavelengths via transfer detectors to the HACR. The relative response determination, the absolute response ties, and final extraction of an overall scale along with its estimated uncertainties, are given in this and the following sections.

This cryogenic bolometer, which holds the IR spectral response scale, consists of a sapphire disk with a heat sensor on one side and a gold-black absorptive coating on the other side. Incident radiation is detected as a temperature rise. Because the bolometer operates by sensing energy deposited within its absorber, its relative response is just the product of the absorptance of the bolometer's coating and the transmittance of the window of the cryogenic Dewar. For more details on the device construction and characterization, see [5-7].

2.1 Bolometer spectral absorptance

The spectral absorptance of the bolometer gold-black coating was measured using a Fourier Transform Infrared (FTIR) spectrometer system with hemispherical collection optics. This allowed the total reflectance (diffuse and specular) to be measured. Two additional measurements were made using laser sources. At

0.633 μm and 10.6 μm, the reflectances were 1.2 ± 0.3 % and 0.5 ± 0.3 %, respectively. (The uncertainties reported in this paper are all standard uncertainties as defined in [8].) The results are shown in Figure 1. A linear fit to the FTIR data from 2 μm to 17 μm indicates a minimal slope with a value not much larger than its uncertainty. Because of this, the FTIR reflectance data were simply averaged yielding a wavelength-independent value for the reflectance of $R = 0.75$ %. This is consistent with the values and uncertainties of the two laser reflectance measurements. As the uncertainty of the absolute value of the FTIR measurements is difficult to ascertain, the uncertainty of the average (which is nearly the same as the average of the laser results) is assigned the value of the laser measurement uncertainties, i.e. 0.3 %. This uncertainty is consistent with the spread of a three-point data set consisting of the two laser measurements and the FTIR average. Because the IR termination of the reflectance data beyond 17 μm resulted from low FTIR sensitivity rather than a variation of gold-black, it is expected that an extrapolation of these data is justified to at least 20 μm.

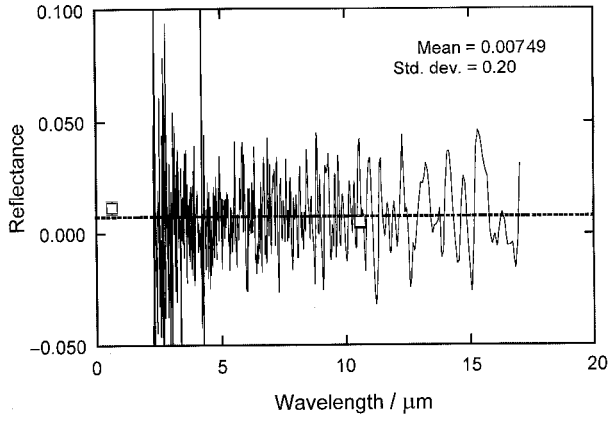

Figure 1. Total bolometer reflectance (specular + diffuse). The solid curve shows the bolometer gold-black reflectance measured using a Fourier Transform Infrared spectrometer. The reflectance was measured with laser sources as indicated by the two open squares at 0.633 μm and 10.6 μm.

This absorptance determination assumes that the transmittance of radiation through the bolometer can be neglected. If this were not the case, a step in the measured reflectance would be seen between 10 μm and 13 μm, as the sapphire substrate reflectance varies rapidly in that region from zero to 100 %. Because no such change is seen in Figure 1, any transmittance must be below the uncertainty of the reflectance measurement. In addition, if radiation were leaking through the bolometer a response increase would be seen at shorter wavelengths owing to non-bolometric effects (caused by direct optical excitation of the Si temperature sensor). There is no evidence of any response change in that spectral range that is not due to window transmittance.

2.2 Bolometer window spectral transmittance

The transmittance of the bolometer window was measured from 600 nm to beyond 18 μm. To accomplish this, several measurement systems were used: the Infrared Spectral Comparator Facility (IR SCF) itself, the Visible Near Infrared Spectral Comparator Facility (VIS/NIR SCF), an FTIR spectrometer, as well as measurements made using laser sources. This allowed for consistency checks of the results. One difficulty in these measurements was caused by the deflection of the transmitted beam produced by the window wedge angle. (A wedged window was used to allow the bolometer to measure laser radiation, as well as incoherent sources. As the bulk absorptance of KBr is unmeasurable in this region with the extinction coefficient below 10^{-6} [9] the variation in window thickness is not a significant source of uncertainty.) The various measurements handled this problem differently.

The IR SCF was used to measure single KBr window samples from 2 μm to 20 μm. Here the deflection of the transmitted beam was handled by repositioning the detector for maximum signal for the window in and out measurements. This should reduce the uncertainty arising from detector spatial nonuniformity to equal or less than the repeatability uncertainty of the measurements. The transmittance is shown in Figure 2a with the error bars being the standard deviation of five to nine repeated measurements. The mean size of the error bars is ~0.1 % for the region from 2 μm to 16 μm. The IR SCF was used to measure the transmittance difference of two window samples (see Figure 2b). The mean difference between the two measurements was 0.016 % with a standard deviation of 0.2 %. These small differences allow window interchanges with this standard deviation used as the uncertainty. They also indicate that the spatial uniformity of the windows, which was not specifically tested, should be significantly below these levels.

Figure 3 shows the transmittance and associated standard deviation for a single sample of KBr measured from 0.6 μm to 1.8 μm by the VIS/NIR SCF. The standard deviation is used as the measurement uncertainty. This VIS/NIR measurement was included because the window transmittance and bolometer response remain relatively flat there and it is frequently convenient to be able to use the bolometer for measurements in this range.

For the window transmittance measurements made by the FTIR spectrometer, an arrangement was made to avoid deflecting the transmitted beam. This was done by measuring the transmission of two windows mounted together so that their wedge angles cancelled out. The transmission of a single piece was then just the square root of the combined transmission. (This assumption is justified by the level of the agreement seen in the IR SCF results shown in Figure 2b). These FTIR results, although less reproducible than the IR

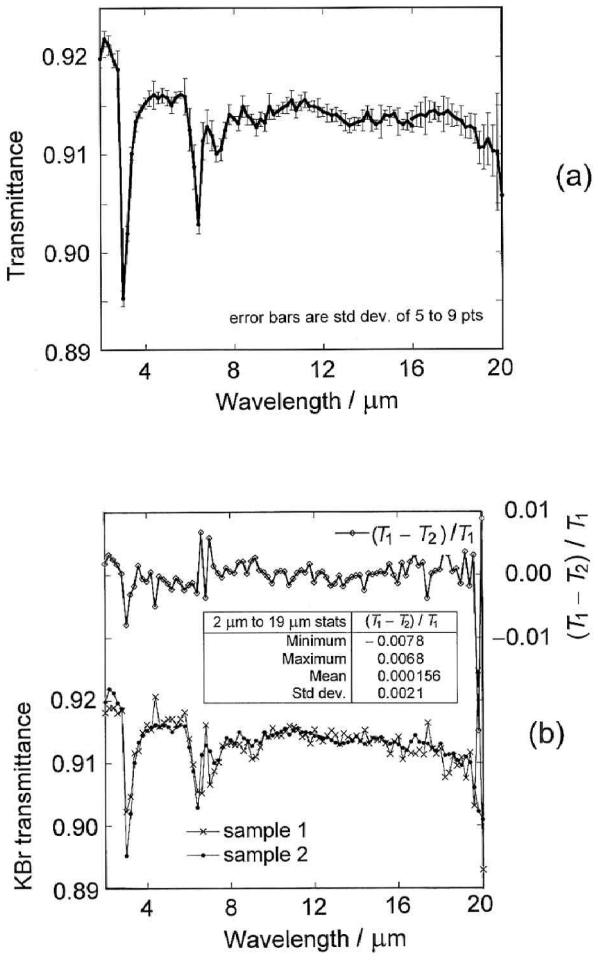

Figure 2. (a) Spectral transmittance of a single KBr window as measured by the Infrared Spectral Comparator Facility. The mean error bar is ~0.1 % for the region below 16 μm. (b) Spectral transmittance of two KBr windows and their relative differences.

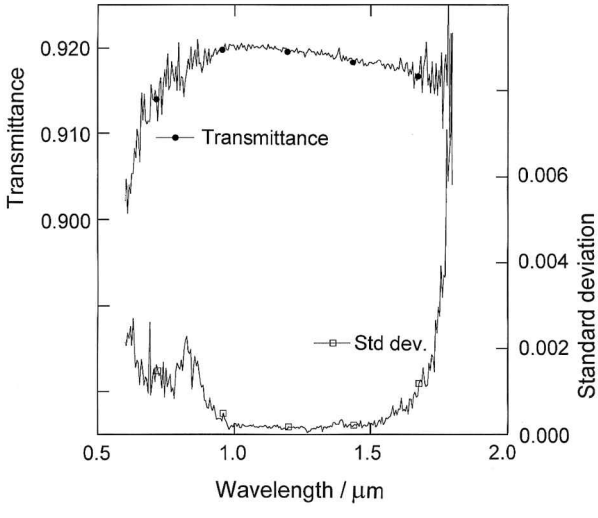

Figure 3. The transmittance of a single KBr window as measured by the VIS/NIR Spectral Comparator Facility. The lower curve is the standard deviation of the transmittance measurements.

SCF measurements, agreed with those results to within 0.2 % to 0.6 %. Because the FTIR is more susceptible to drifts than the IR SCF measurements and because the FTIR can be sensitive to alignment in a way that is difficult to quantify, we used the IR SCF measurements of the window transmittance.

An attempt was made to determine the KBr transmittance by measuring just the reflected beams from the front and back window surfaces. This would have had the advantage of allowing window transmittance to be measured *in situ* on the Dewar. Unfortunately the method yielded inconsistent results and was not pursued. It was suspected that the problem arose from surface scatter or surface absorptance.

2.3 Relative response result

The relative spectral response of the bolometer as shown in Figure 4 is the product of the window transmittance and the bolometer gold-black absorptance. Except for a pair of 1 % to 2 % dips (most likely from window-coating absorption lines) the bolometer response is quite flat. The uncertainty for the 2 μm to 20 μm region is 0.36 %, the quadrature sum of the 0.2 % KBr transmittance uncertainty and the 0.3 % gold-black absorptance uncertainty. In the 0.6 μm to 2 μm region the transmittance uncertainty is so small that the gold-black absorptance uncertainty dominates the total uncertainty.

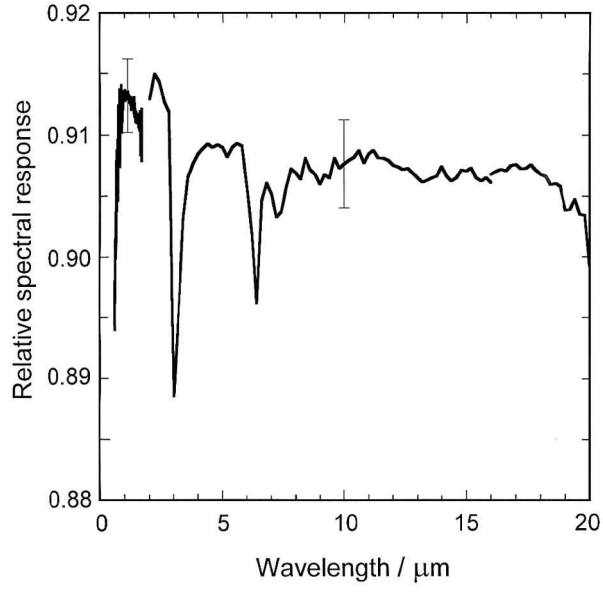

Figure 4. Relative spectral response of the bolometer (window transmittance × gold-black absorptance) with uncertainties typical of the VIS/NIR and IR spectral regions.

3. Absolute response tie points

To convert the relative spectral curve just discussed into an absolute scale it is necessary to determine the absolute response at one, or preferably more,

wavelengths. This was done by comparison with Si, Ge, and pyroelectric transfer standard detectors, which were themselves tied to the HACR primary standard. The comparisons were made at specific wavelengths using laser sources at 0.633 μm, 1.3 μm, and 10.6 μm and over a continuous range from 600 nm to 900 nm using the quartz lamp and the IR SCF itself as the source. Even though the VIS/NIR calibrations are outside the intended range of the IR SCF, these measurements are important because of their accuracy and to verify the spectral flatness of the bolometer.

3.1 Infrared transfer: pyroelectric detector

The bolometer was compared with a pyroelectric transfer detector over a continuous spectral range from 6 μm to 11 μm using the IR SCF. This pyroelectric detector was calibrated against the HACR at a single wavelength of 10.6 μm using a laser source [10]. To extend the calibrated spectral range of this transfer detector, a response comparison was made between it and a second pyroelectric detector that did not have an absolute calibration but had a known relative spectral response. This comparison was performed on the IR SCF. Because it was windowless, the relative response of this second detector was found by measuring the total reflectance of its absorptive coating in the infrared using an FTIR spectrometer. This procedure yielded the spectral response of the pyroelectric transfer detector as shown in Figure 5. The overall decrease in response with increasing wavelength is a result of decreasing absorptance of the coating on the pyroelectric detector.

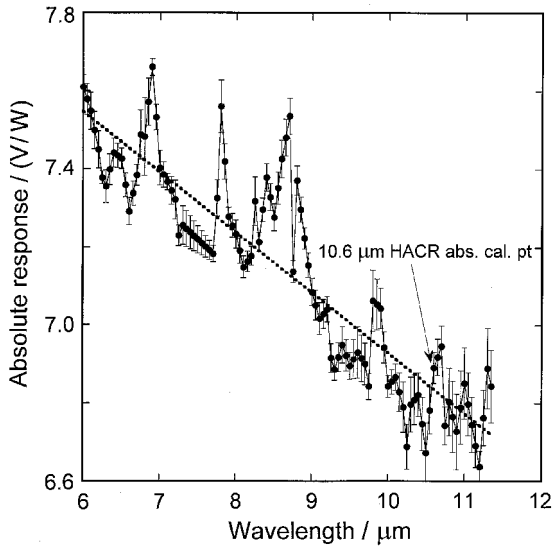

Figure 5. The radiant power response of the pyroelectric detector used for scale transfer from the High Accuracy Cryogenic Radiometer (HACR) to the bolometer. The absolute tie point to the HACR at 10.6 μm is indicated. A linear fit to the data is shown.

The comparison of the bolometer with the pyroelectric transfer detector determined the bolometer response over the 6 μm to 11 μm spectral range as shown in Figure 6. This result combines three comparisons made over different wavelength ranges. Table 1 shows the typical component uncertainties associated with this bolometer response calibration. The top portion of the table contains the uncertainties associated with the bolometer response corrections and signal handling. As indicated by the subtotals attributed to each detector, the pyroelectric detector uncertainty dominates the uncertainty of this comparison. The lower portion of the table contains the uncertainties associated with the pyroelectric measurements and pyroelectric response scale. The λ uncertainty component derives from the wavelength uncertainty of the monochromator combined with the slope of the pyroelectric detector response versus wavelength. The final total uncertainty for the bolometer response contains all the listed components combined in quadrature with the pyroelectric response scale uncertainty which dominates the result. The pyroelectric response scale uncertainty is flat at 1 % from 6 μm to 9 μm and then smoothly rises to ~1.6 % at 11 μm.

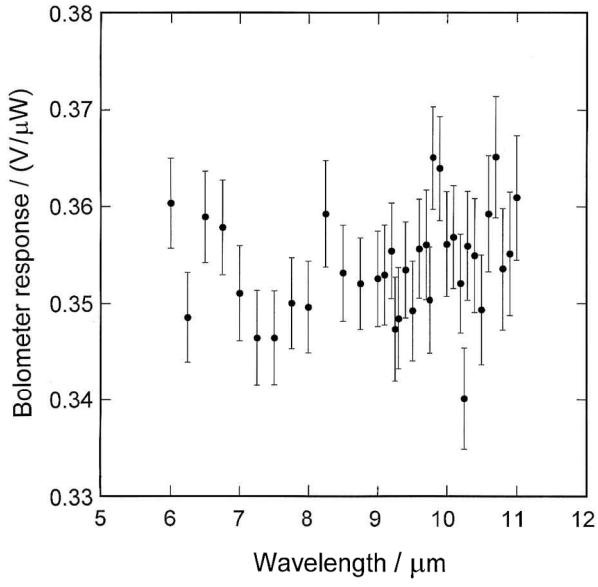

Figure 6. Bolometer spectral radiant power responsivity as transferred using the pyroelectric detector. Error bars are total uncertainty including all components shown in Table 1.

3.2 Near-infrared transfer: Ge detector

The bolometer was compared with a Ge transfer detector over a continuous spectral range from 0.9 μm to 1.7 μm using the IR SCF. (These Ge measurements, as well as the Si measurements described in the next section, required replacing the usual IR gratings in the monochromator with a 600 g/mm grating.) This transfer detector is tied to the HACR from 0.8 μm to 1.8 μm via a calibration chain that includes single-element and

Table 1. Uncertainty budget for the bolometer spectral radiant power responsivity in the wavelength range 6 μm to 11 μm, as transferred from the pyroelectric detector.

Correction factors and uncertainty sources	C	$100 \times (\Delta C/C)$	Wavelength dependency
$C_{f_{3dB}}(f)$	1.1325	0.29	Varies
C_{V_d}	1.3611	0.19	Varies
V_{bias}	1.0189	0.10	Varies
$G_{20\rightarrow100}$	4.9669	0.18	Fixed
C_{NL}	1.0482	0.27	Varies
$C_{\text{lock-in output-gain}}$	0.9865	0.55	Fixed
$C_{\text{lock-in input-gain}}$ ($G_{\text{lock-in}} = 10^4$)	1.0032	0.21	Fixed
Bolometer signal noise		0.05	Varies
Bolometer spatial response		0.3	Fixed
Bolometer total		0.79	
Pyroelectric scale		1.18 at 10 μm	Varies
λ uncert. ($\Delta\lambda$ = 1.5 nm)		0.02 at 10 μm	Varies
Pyroelectric signal		0.61	Varies
Pyroelectric total		1.33	Varies
Grand total		1.51	

The bolometer response correction factors listed are: $C_{f_{3dB}}$ for the bolometer 3dB frequency point; C_{V_d} for the voltage drop across the bolometer; V_{bias} is the bolometer bias voltage; $G_{20\rightarrow100}$ is the gain of the bolometer preamplifier; C_{NL} is a correction for nonlinearity; $C_{\text{lock-in input-gain}}$ and $C_{\text{lock-in output-gain}}$ are corrections of the lock-in amplifier input and output gains used with the measurement system. The spatial response term assumes a ~1 mm spot centred on the bolometer to within ~0.5 mm. The λ uncert. term arises from the wavelength uncertainty of the IR SCF. For a detailed discussion of these terms see NIST Special Publication 250-42 [11]. The last column indicates whether the uncertainty is constant over a spectral scan or varies between wavelength points.

trap-configuration Si detectors, a pyroelectric detector, and the VIS/NIR SCF [12]. The resulting bolometer response is shown in Figure 7b. The data (indicated by solid circles) show the comparison from 0.9 μm to 1.8 μm that was made at a gain chosen to avoid saturation at the peak Ge signal. The second comparison from 1.5 μm to 1.8 μm (indicated in Figure 7b by open triangles) was made with five times larger gain for improved signal-to-noise ratio, although the two curves show few significant differences. Typical values for the component uncertainties are shown in Table 2 with the total being the quadrature sum. The uncertainties associated with the bolometer are shown in the upper portion of the table and those associated with the Ge measurement and Ge response scale are shown in the lower portion. The final total uncertainty for the bolometer response contains all the listed components combined in quadrature with the

Table 2. Uncertainty budget for the bolometer spectral radiant power responsivity as transferred from the Ge detector.

	0.9 μm to 1.8 μm		1.5 μm to 1.8 μm		1.31 μm		
Correction factors and uncertainty sources	C	$100 \times (\Delta C/C)$	C	$100 \times (\Delta C/C)$	C	$100 \times (\Delta C/C)$	Wavelength dependency
$C_{f_{3dB}}(f)$	1.1014	0.05	1.1134	0.10	1.1184	0.05	Varies
C_{V_d}	1.3959	0.47	1.3987	0.18	1.4807	0.07	Varies
V_{bias}	1.0189	0.03	1.0197	0.01	1.0122	0.01	Varies
$G_{X\rightarrow100}$	0.4930	0.03	0.4930	0.03	1	0	Fixed
	$X = 200$		$X = 200$		$X = 100$		
C_{NL}	1.0004	0.00	1.0026	0.02	1.0042	0.03	Varies
$C_{\text{lock-in output-gain}}$	0.9865	0.55	0.9865	0.55	0.9908	0.55	Fixed
$C_{\text{lock-in input-gain}}$ ($G_{\text{lock-in}}$)	1	0	1	0	1	0	Fixed
Bolometer signal noise		0.03		0.02		0.03	Varies
Bolometer spatial response		0.3		0.3		0.3	Fixed
Bolometer total		0.79		0.66		0.63	
Ge scale		1.30 at 1.3 μm		2.83 at 1.5 μm		1.30 at 1.3 μm	Varies
λ uncert. ($\Delta\lambda$ = 1.5 nm)		0.16 at 1.3 μm		0.06 at 1.5 μm		0.16 at 1.3 μm	Varies
Ge signal		0.14		0.00		0.19	Varies
Ge total		1.32		2.83		1.32	
Grand total		1.56		2.93		1.47	

The last column indicates whether the uncertainty is constant over the spectral range or varies with wavelength.

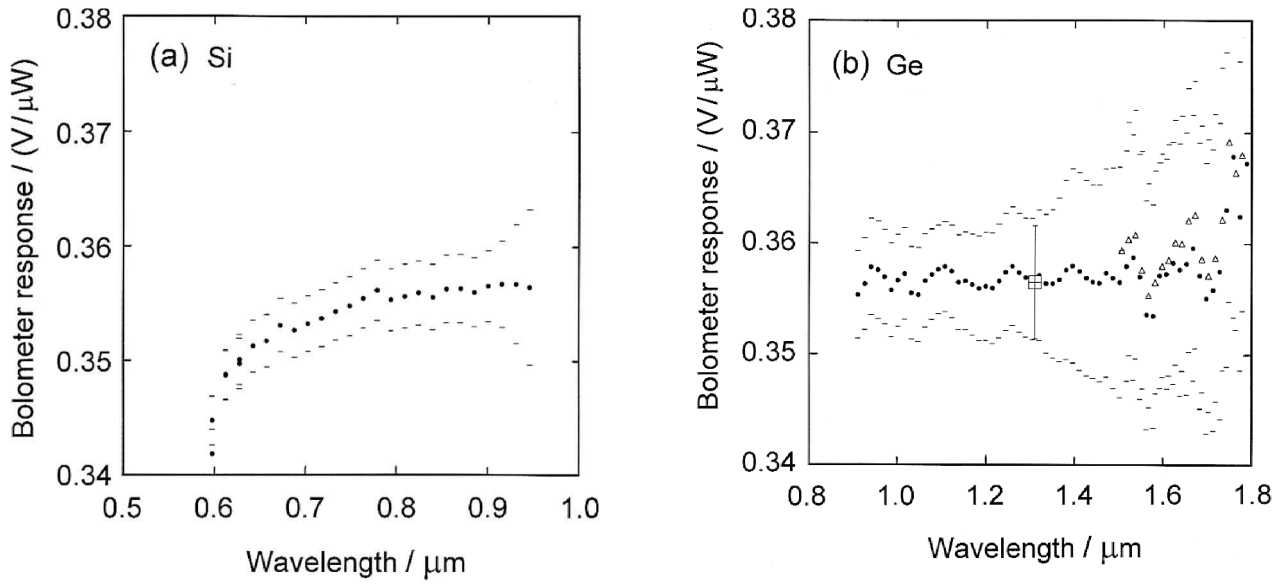

Figure 7. Bolometer response calibration by comparison with (a) Si and (b) Ge transfer standard detectors. The response is to power incident on the chopper. Only the error-bar caps are shown for clarity except for the Ge comparison point, which was made using the 1.31 μm laser as a source instead of the IR Spectral Comparator Facility.

Table 3. Uncertainty budget for the bolometer spectral radiant power responsivity in the wavelength range 0.6 μm to 0.95 μm as transferred from the Si detector.

Correction factors and uncertainty sources	C	$100 \times (\Delta C/C)$	Wavelength dependency
$C_{f\,3dB}\,(f)$	1.1062	0.10	Varies
C_{Vd}	1.4024	0.19	Varies
V_{bias}	1.0194	0.11	Varies
$G_{200\rightarrow100}$	0.4930	0.03	Fixed
C_{NL}	1.0000	0.00	Varies
$C_{lock\text{-}in\ output\text{-}gain}$	0.9865	0.55	Fixed
$C_{lock\text{-}in\ input\text{-}gain}\ (G_{lock\text{-}in})$	1	0	Fixed
Bolometer signal noise		0.06	Varies
Bolometer spatial response		0.3	Fixed
Bolometer total		0.68	
Si scale		0.11	Fixed
λ uncert. (Δλ = 1.5 nm)		0.19 at 0.8 μm	Varies
Si signal		0.06	Varies
Si total		0.23	
Grand total		0.71	

The last column indicates whether the uncertainty is constant over the spectral range or varies with wavelength.

Ge response scale uncertainty, which dominates the result. The Ge response scale uncertainty ranges from slightly less than 1 % from 0.8 μm to 1.1 μm and then smoothly rises to ~3 % at 1.7 μm.

In addition to the continuous NIR spectral calibration made using the IR SCF, the absolute bolometer response was measured at 1.31 μm by comparison with the Ge standard using a diode laser source. The comparison was performed by repeatedly swapping bolometer and Ge detector into and out of the laser beam. The laser power as seen by the Ge detector was stable to ±0.5 % during this comparison, which yielded an absolute bolometer response of 0.3565 V/μW with the uncertainty given in Table 2. From the subtotals, it can be seen that it was the uncertainty of the Ge detector that dominates the uncertainty of the bolometer-Ge comparison.

3.3 Visible transfer: Si detector

For added redundancy and because the bolometer response is flat down to ~0.6 μm, the bolometer response was compared with a Si photodiode from 0.6 μm to 0.95 μm, with the results shown in Figure 7a. This transfer detector is tied to the HACR from 0.4 μm to 0.9 μm via a calibration chain that includes single-element and trap-configuration Si detectors and the VIS/NIR SCF [12, 13]. The uncertainties of this comparison are given in Table 3. For this comparison, the bolometer uncertainty dominates the overall result with the lock-in gain calibration uncertainty being the largest component. This differs from the Ge and pyroelectric comparisons, in which the transfer detector scale uncertainties dominated.

4. Overall bolometer absolute spectral response, calibration and scale uncertainty

The overall bolometer spectral response is shown in Figure 8, where it is overlaid on the predicted response calculated from the bolometer reflectance and window transmittance. This prediction is a relative spectral curve, requiring a single scale factor to fit all of the absolute measurements. The predicted curve shown is $T \times (1 - R)$ 0.3913 V/μW. As may be seen from

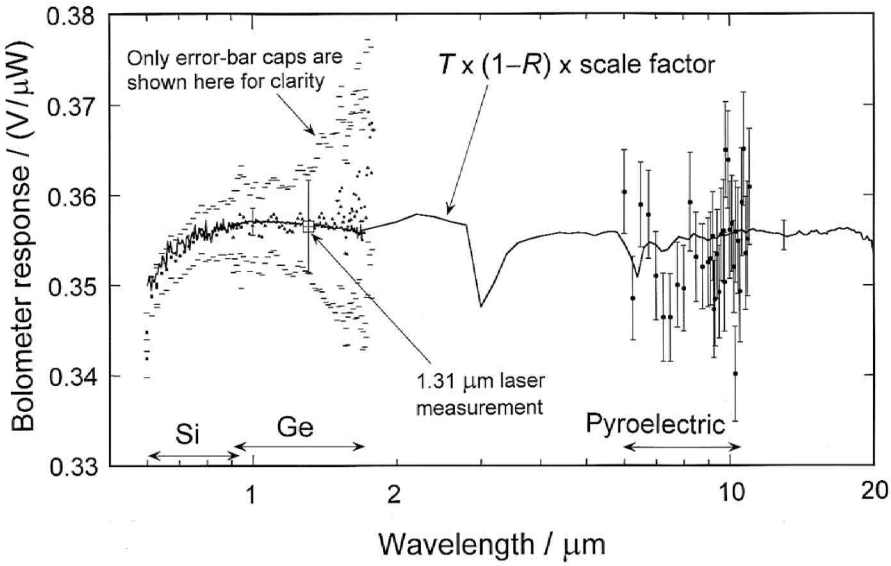

Figure 8. The radiant power response of the bolometer in the spectral regions tied to the Si and Ge transfer standard detectors are indicated by the solid points between 0.6 μm and 1.8 μm. For clarity, only the error-bar caps are given for these points. The response measurement made using a diode laser at 1.31 μm is indicated by the box and error bar. The bolometer response tied to the pyroelectric transfer detector is indicated by the points between 6 μm and 11 μm with error bars. The solid curve is the $T \times (1 - R)$ relative response, scaled by a constant factor to give the best overall fit. The two uncertainty error bars for the $T \times (1 - R)$ curve shown at 1 μm and 12 μm arise from the uncertainty of the relative spectral data and the spatial response uncertainty of the bolometer.

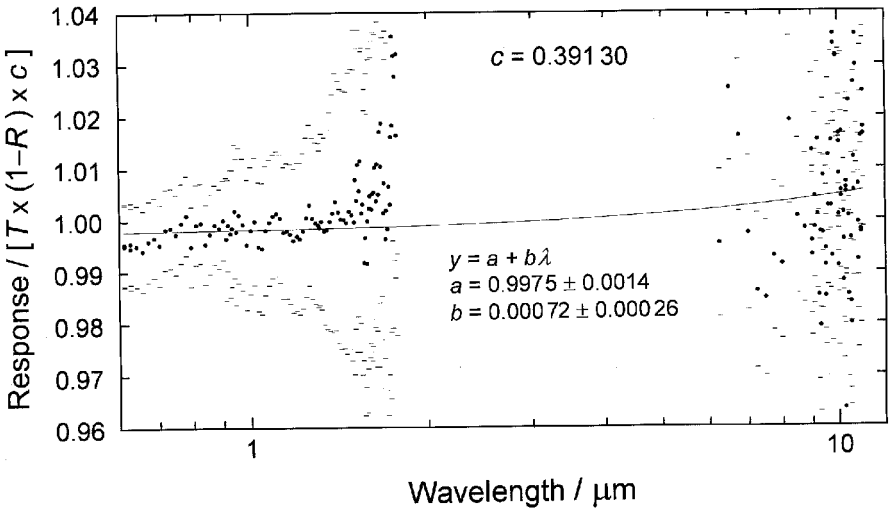

Figure 9. Ratio of the absolute bolometer radiant power response to the scaled relative response. The error bars indicate the total uncertainty of the ratios; to improve clarity, only the error-bar caps are shown. The solid line is the fit to a line; the uncertainties were assumed to be statistical for this fit.

the figure, the predicted response is a good fit, well within the uncertainties. For the VIS/NIR region the data show excellent smoothness reflecting the quality of the Si and Ge transfer standards. The IR region shows much higher variation owing to the poorer quality of the pyroelectric transfer detector, which had a much lower signal-to-noise ratio, poorer spatial response uniformity, and involved a more difficult calibration transfer. The overall fit of the predicted curve shape to the actual measurements over the 0.6 μm to 11 μm range indicates good self-consistency. This should be emphasized as the overall data set includes three independent transfer detectors and a continuous spectral source as well as a laser source. This good self-consistency increases confidence in the regions where absolute measurements were not made and the response predictions must be relied upon.

The overall scale factor of the relative response curve was determined by taking the ratio of the bolometer response to the predicted relative response

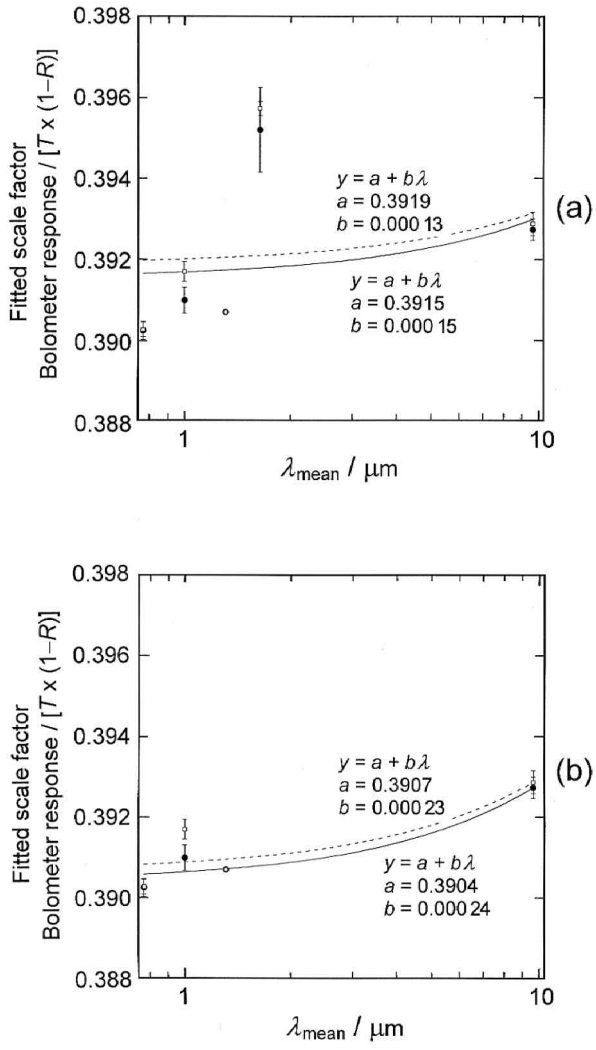

Figure 10. Relative response curve scale factors were determined for individual data runs. The scale factors from those runs were then fitted versus wavelength. The solid circles indicate results assuming all uncertainty components are statistical. For the open squares only the statistical uncertainty components were used in the weights for the fits. (The error bars indicate the uncertainties used for each fit.) The solid and dashed lines indicate the fit to the solid circles and open squares, respectively. All data sets are shown in (a), while the noisy 1.5 μm to 1.7 μm data set has been removed from (b).

$T \times (1 - R)$. The weighted mean of all the ratio data was $0.3913 \pm 0.000\,15$ (the uncertainty is the standard deviation of the mean). The weights used were the ratio uncertainty (the quadrature sum of the uncertainties of the response measurements and the response curve). This constant is a scale factor to convert the relative response curve to an absolute scale. All uncertainty components were included, so the non-statistical uncertainty correlations are ignored here. This analysis assumes a single scale factor over the entire wavelength range. To test this, the ratios of the response measurements to the now absolute predicted response were plotted versus wavelength and fitted to a line. As shown in Figure 9, the fit stays within 0.25% of unity, indicating that any systematic tilting of the relative curve is less than this value.

To test the effect of neglecting correlation in the uncertainties, a second analysis was made where individual data sets were averaged separately and the individual scale factors plotted versus the mean wavelength of the set. Because an individual data set used only a single transfer standard, uncertainty components arising from the transfer standard are likely to be correlated. To test the size of the effect on the net scale factor, two sets of weights were used. One used only the uncertainty components that are statistical, while the second used the total uncertainties of each point. The resulting scale factors of each data set are shown in Figure 10. The differences between the two methods are ± 0.25 % or less. The fits of these scale factors versus wavelength are similar to the result of treating all of the data points as a single set.

Taken together, these different analysis schemes support an overall uncertainty of ± 0.25 % in the absolute response scale given by the relative response, scaled by a factor of 0.3913, shown as the solid curve in Figure 8. This uncertainty when combined with the uncertainty associated with a bolometer radiant power measurement at a specific wavelength (~0.75 % from Tables 1 to 3) gives an overall bolometer radiant power scale uncertainty of ~0.8 %. This is the uncertainty that can be expected for a bolometer measurement of radiant power made at a single wavelength within the 2 μm to 20 μm range of the IR SCF (assuming adequate measurement time is allowed so as not to be limited by bolometer signal noise). This uncertainty is comparable with the quoted uncertainty of a similar IR scale also set up for detector calibrations [3].

In conclusion, the NIST has implemented an IR spectral radiant power scale on a cryogenic bolometer. This scale will be used to provide IR detector calibrations using NIST's IR SCF over the range 2 μm to 20 μm. The uncertainty is comparable with the best existing IR scales. It is believed that this bolometer is the most sensitive detector used for a scale realization over this spectral range.

References

1. Migdall A. L., Eppeldauer G., Cromer C. L., *Cryogenic Optical Systems and Instruments VI, Proc. SPIE*, 1994, **2227**, 46-53.
2. Parr A. C., *A National Measurement System for Radiometry, Photometry, and Pyrometry Based upon Absolute Detectors*, NIST Technical Note 1421, 1996.
3. Nettleton D. H., Prior T. R., Ward T. H., *Metrologia*, 1993, **30**, 425-432.
4. Gentile T. R., Houston J. M., Cromer C. L., *Appl. Opt.*, 1996, **35**, 4392-4403.
5. Eppeldauer G., Migdall A. L., Cromer C. L., *Metrologia*, 1993, **30**, 317-320.

6. Eppeldauer G., Migdall A. L., Gentile T. R., Cromer C. L., *Photodetectors and Power Meters II, Proc. SPIE*, 1995, **2550**, 36-46.
7. Eppeldauer G., Migdall A. L., Cromer C. L., *Thermal Phenomena at Molecular and Microscales and in Cryogenic Infrared Detectors* (Edited by M. Kaviany et al.), New York, ASME HTD-Vol. 277, 1994, 63-67.
8. Taylor B. N., Kuyatt C. E., *Guidelines for Evaluating and Expressing the Uncertainty of NIST Measurement Results,* Natl. Inst. Stand. Technol. (US), Tech. Note 1297, 1994 ed.
9. Palik E. D., *Handbook of Optical Constants of Solids II*, Boston, Academic Press, 1991, 993.
10. Gentile T. R., Houston J. M., Eppeldauer G., Migdall A. L., Cromer C. L., *Appl. Opt.*, 1997, **36**, 3614-3621.
11. Migdall A. L., Eppeldauer G., *Spectroradiometric Detector Measurements: Part III – Infrared Detectors,* Natl. Inst. Stand. Technol. (US), Spec. Publ. 250-42, in preparation (1998).
12. Larason T. C., Bruce S. S., Parr A. C., *Spectroradiometric Detector Measurements: Parts I and II – Ultraviolet and Visible to Near Infrared Detectors*, Natl. Inst. Stand. Technol. (US), Spec. Publ. 250-41, 1998.
13. Larason T. C., Bruce S. S., Cromer C. L., *J. Res. Natl. Inst. Stand. Technol.*, 1996, **101**, 133-140.